JACS
JOURNAL OF THE AMERICAN CHEMICAL SOCIETY
Article
pubs.acs.org/JACS

Decarboxylative Polymerization of 2,6-Naphthalenedicarboxylic Acid at Surfaces

Hong-Ying Gao,*[,†,‡] Philipp Alexander Held,[§] Marek Knor,[†,‡] Christian Mück-Lichtenfeld,[§,∥] Johannes Neugebauer,[§,∥] Armido Studer,*[,§] and Harald Fuchs*[,†,‡,∥,⊥]

[†]Center for Nanotechnology, Heisenbergstraße 11, 48149 Münster, Germany

[‡]Physikalisches Institut, Westfälische Wilhelms-Universität, Wilhelm-Klemm-Straße 10, 48149 Münster, Germany

[§]Organisch-Chemisches Institut and [∥]Center for Mutiscale Theory and Simulation, Westfälische Wilhelms-Universität, Corrensstraße 40, 48149 Münster, Germany

[⊥]Institute for Nanotechnology, Karlsruhe Institute of Technology, 76344 Karlsruhe, Germany

Supporting Information

ABSTRACT: Metal-catalyzed polymerization of 2,6-naphthalenedicarboxylic acid (NDCA) to form poly-2,6-naphthalenes at various surfaces is reported. Polymerizations occur via initial formal dehydrogenation of self-assembled diacids with subsequent decarboxylation to give polymeric bisnaphthyl-Cu species at elevated temperature as intermediate structures (<160 °C). Further temperature increase eventually leads to poly-naphthalenes via reductive elimination. It is demonstrated that the Cu(111) surface works most efficiently to conduct such polymerizations as compared to the Au(111), Ag(111), Cu(100), and Cu(110) surfaces. Poly-2,6-naphthalene with a chain length of over 50 nm is obtained by using this approach. The decarboxylative coupling of aromatic diacids is a very promising tool which further enlarges the portfolio of reactions allowing for on-surface polymerizations and novel organometallic systems preparations.

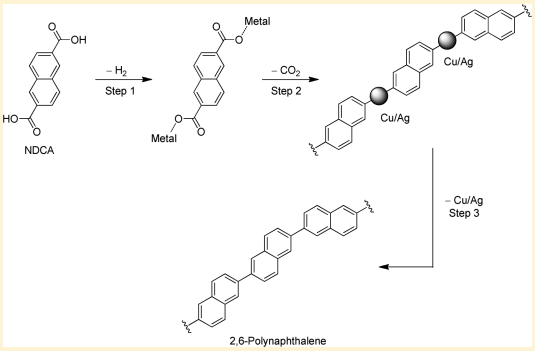

1. INTRODUCTION

Bottom-up covalent assembly of molecular building blocks, carrying specific functions, at surfaces has recently emerged as a very active field of research.[1−7] Remarkably, several reliable chemical reactions have been developed for preparing various fascinating nanostructures: Ullman coupling,[8−14] imine formation,[15−17] dehydration of boronic acids,[18] dimerization of N-heterocyclic carbenes,[19] acylation reactions,[20,21] cycloaddition,[22−24] and dehydrogenations.[25−29] STM studies provided detailed insight at the single-molecule level on these reactions by identifying reaction intermediates. However, the effect of the substrate on these reactions has not been well explored, which is of fundamental importance for understanding and controlling on-surface chemical processes. To our knowledge, only for the Ullman coupling[14,30,31] and the Glaser coupling large differences exerted by the substrate on the coupling reaction have been reported. Although great progress in on-surface chemistry has been achieved over the past few years, novel reaction types and accordingly reaction paths must be designed which may allow the preparation of even more complex structures at the surface.

Reaction design based on carboxylic substituents as reactive functionalities should be a promising approach, because the interaction between the COOH group and surface can be steered by the reduction−oxidation ability of the metal. Moreover, aromatic carboxylic acids should form well-ordered self-assembled structures upon ultrahigh vacuum deposition at surfaces, and it is known that the metal can mediate self-assembly. For example, metal−organic coordinated networks of carboxylic groups at metal surfaces (via codepositing molecules with metal atoms onto surfaces) have been reported and formation of metal carboxylates by Fe/Cu has been observed in a few cases.[3,32] Based on these important findings several interesting questions arise: (1) Can the carboxyl (COOH) group be applied as reactive functionality for on-surface decarboxylative C−C coupling reactions? (2) What is the effect of the substrate on the C−C coupling process? (3) Can the on-surface reaction be used for two-dimensional polymerization if arene dicarboxylic acids are applied as substrates and can polymerization be controlled and used to build up larger linear structures?[33]

Along these lines, we decided to test 2,6-naphthalenedicarboxylic acid (NDCA) as a precursor for the construction of polymer chains. By characterization of reaction intermediates we will show that C−C coupling occurs via a stepwise process (Scheme 1). The carboxyl functionality first reacts with metal atoms at the surface in a dehydrogenation process to provide

Received: April 11, 2014
Published: June 17, 2014

dx.doi.org/10.1021/ja5033875 | J. Am. Chem. Soc. 2014, 136, 9658−9663

Scheme 1. (a) Schematic Illustration of the Reaction Pathways of Metal-Catalyzed on-Surface Polymerization of NDCA and (b) Corresponding Reaction Equation

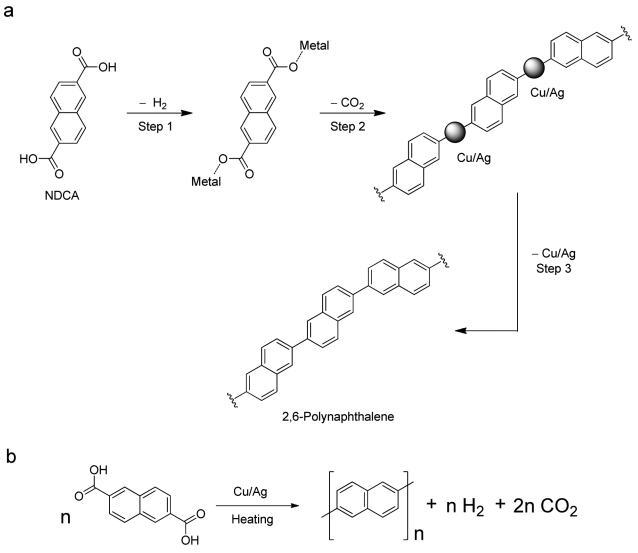

the corresponding metal carboxylate, as previously reported[32] (step 1). Increase of temperature will lead to polymeric bisnaphthyl-Cu as intermediate structures by decarboxylative processes (step 2). Further increase of temperature eventually generates poly-2,6-naphthalene chains via decarboxylation. Note that the decarboxylative C−C coupling using aryl carboxylic acids as aryl metal precursors is an established reaction in homogeneous catalysis;[34] however, this process has not been adapted to the emerging research area of on-surface chemistry. By varying the substrate, catalysis efficiency of the surface for decarboxylative coupling was studied. Individual precursors, reaction intermediates and final products are readily monitored by scanning tunneling microscopy (STM).

2. RESULTS AND DISCUSSION

Reductive Coupling of NDCAs at Ag(111) Surface. Our initial studies were performed on the Au(111) surface. Figure 1b depicts a representative STM image with NDCAs on Au(111). In the image we identified linearly assembled NDCAs where the individual acid moieties are connected by hydrogen bonding. In the H-bonded NDCA structures we found both R- and L-chiral NDCAs as shown in the red dashed rectangle (Figure 1b zoom-in image; see also chemical structure in Figure 1d. Assignment of chirality is mainly based on STM image analysis by superposition of the chemical structure of NDCA; the two carboxylic acid moieties always appear bright in the image at the opposite corners of the individual entities). The molecule center-to-center distance between NDCAs was measured to be 1.24 ± 0.01 nm at the Au(111) surface (see Figure 1d). Interestingly, no significant difference with respect to center-to-center distance was observed in homo and heterochiral arrangements: similar values were measured for R-to-R (L-to-L) and R-to-L NDCA distances.

We next attempted to induce on-surface reaction by thermal annealing. However, neither metalation of the carboxylic acids nor any covalent coupling was observed after thermal treatment (132 °C for 30 min). Only phase transition of the self-assembly structures and desorption phenomena were noted (see Supporting Information, SI-Figure 1). We assume that the

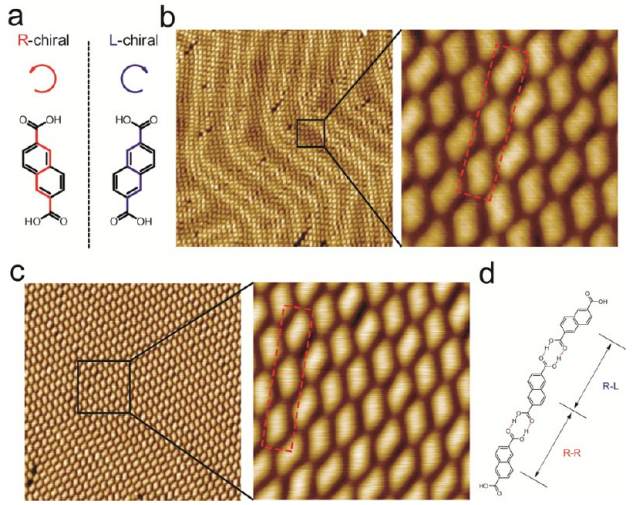

Figure 1. Self-assembly structure of NDCAs via hydrogen bonding at surfaces. (a) Molecular structure of the NDCA with R- and L-chirality at the metal surface. (b and c) Representative STM images (b, 40 × 40 nm; c, 25 × 25 nm) and their high-resolution images (b, 5 × 5 nm; c, 6 × 6 nm) of NDCA acids in the self-assembly structure via hydrogen bonding at the Au(111) and Ag(111) surface, respectively (Au(111): b, −0.5 V, 100 pA; Ag(111): c, −0.1 V, 100 pA). (d) Chemical structure of a hydrogen-bonded NDCA trimer with R, R and L-chirality.

interaction of the COOH group with the Au(111) surface is too weak to induce any reaction. Therefore, we switched to the Ag(111) surface, which should show a stronger interaction with the carboxyl groups according to the increasing reduction−oxidation ability of noble metals from Au to Ag to Cu. The NDCA self-assembly structure via hydrogen bonding on Ag(111) was similar to the structure obtained on Au(111) (Figure 1c). Notably, the NDCA center-to-center distance was 1.34 ± 0.01 nm, which is 0.1 nm larger than on the Au(111) surface. We believe that this is due to the stronger confinement of the Au(111) surface due to its herringbone reconstruction, indicating that hydrogen-bonding length depends on the substrate, as reported.[35]

After thermal annealing at 156 °C we found that covalent coupling of NDCAs occurred at Ag(111). Figure 2a-i shows a representative STM image containing some reacted NDCA oligomers and also unreacted NDCA molecules in a new self-assembly phase. Due to the R- and L-chirality of surface adsorbed NDCAs, two types of conjugations were experimentally observed designated as type 1 (R-to-R or L-to-L, homochiral conjugations) and type 2 (R-to-L, heterochiral conjugations). The center-to-center distance for R−R (L−L) conjugations was measured to be 0.95 ± 0.03 nm, while the R−L center-to-center distance was 0.90 ± 0.03 nm. We suggest oligomeric structures where an Ag atom connects two naphthyl moieties (C−Ag−C) for these intermediates, because distances for such organometallic polymeric structures agree very well with theoretical calculated distances (0.936 nm for R−R case (NaphthylAg(I)Naphthyl), 0.929 nm for R−L case, more details see SI-Figure 2) (Figure 2a-iii). As expected, the C−Ag−C linkage appears with higher contrast (Figure 2a-ii). The chemical structures of type 1 and type 2 C−Ag−C conjugations are depicted in Figure 2a-iii.

Interestingly, we observed follow up chemistry of the poly-bisnaphthyl-Ag intermediates upon further annealing to 176 °C (Figure 2b-i). At this temperature, the unreacted monomers

dx.doi.org/10.1021/ja5033875 | J. Am. Chem. Soc. 2014, 136, 9658−9663

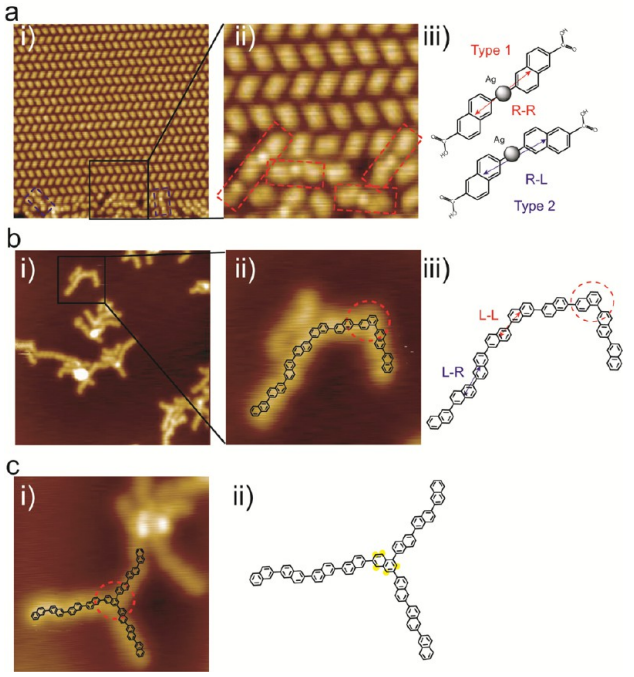

Figure 2. Covalent coupling reactions of NDCAs at Ag(111) surface. (a) STM image (a-i, 20 × 20 nm) and its zoom-in image (a-ii, 6 × 6 nm) of the chemical products of NDCAs on Ag(111) surface after annealing up to 156 °C (−0.05 V, 100 pA). (a-iii) Chemical structures of the bisnaphthyl-Ag species formed by the decarboxylative process of NDCAs. (b) Typical STM image (b-i, 25 × 25 nm) and its high-resolution image (b-ii, 6 × 6 nm) of C−C coupling products of NDCAs on Ag(111) after annealing up to 176 °C (−2 V, 50 pA), and (b-iii) the corresponding chemical structure of the final products. (c) STM high-resolution image (c-i, −2 V, 50 pA, 7.5 × 7.5 nm) of branching conjugation in the products as well its corresponding chemical structure (c-ii).

completely desorbed and short oligomers without higher contrast at the conjugation regions remained at the surface, as shown in Figure 2b-ii. The center-to-center distance was measured as 0.66 ± 0.03 nm for both R-to-R (L-to-L) and R-to-L covalent coupling cases, which is much shorter than for the intermediate bisnaphthyl-Ag species. We assume that upon annealing C−C covalent coupling between naphthalene moieties occurred via reductive elimination of the oligo-bisnaphthyl-Ag intermediate to give oligo-2,6-naphthalene chains. The corresponding chemical structure of the oligo-2,6-naphthalene is shown in Figure 2b-iii. The calculated center-to-center distance for the bisnaphthyl model compound was 0.655 nm which fits very well with the experimentally determined value (SI-Figure 2). STM manipulation on the oligomeric product structures provided strong evidence for the covalent nature of the conjugation of the naphthalene units (SI-Figure 3). In addition, we identified branching conjugations in the final oligomers, for which a representative case is presented in Figure 2c-i. The corresponding chemical structure is depicted in Figure 2c-ii. This finding indicates that arene CH bonds of the naphthalene moiety can also be activated under the applied conditions.

Polymerization of NDCAs at Cu(111) Surface. To further enhance the interaction between the carboxyl groups of NDCA and surface, we tested the Cu(111) surface (Cu is more readily oxidized and will likely show stronger interactions with the carboxyl groups). As expected, a hydrogen-bonded self-assembly structure was also formed at the Cu(111) surface at room temperature (no isolated NDCAs were observed, except at the terrace edges). We identified three different regimes: a disordered phase A, an ordered phase B, and a mixed phase where A and B coexist, as shown in Figure 3a-i. In the high-resolution STM image of phase B, we found the periodic

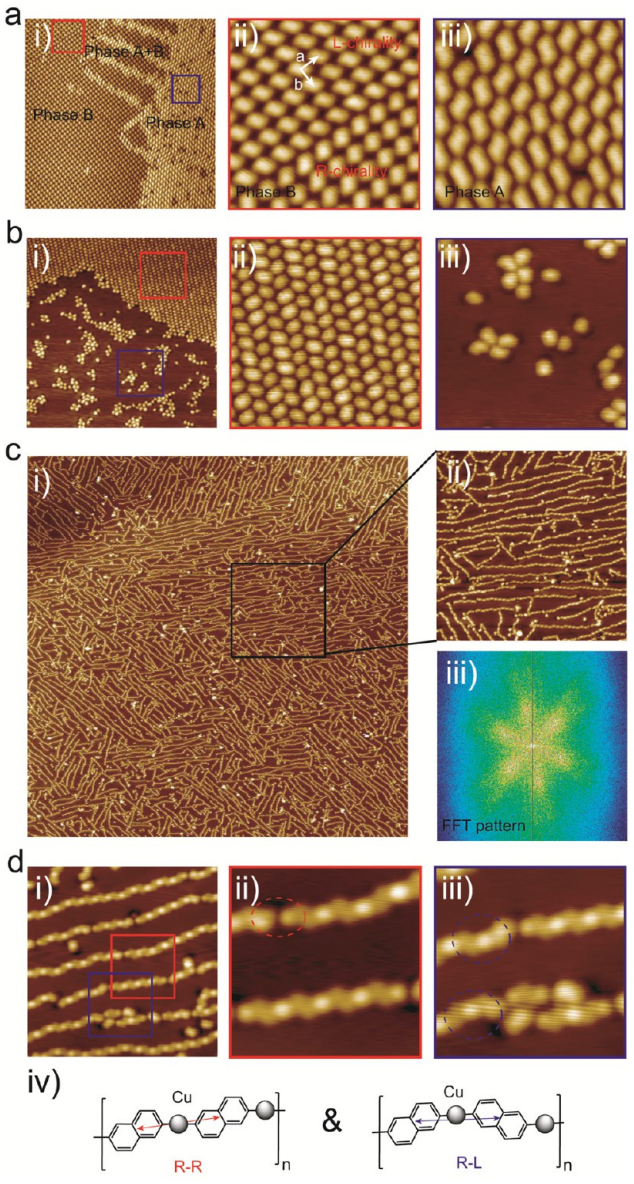

Figure 3. Metallic polymerization of NDCAs at Cu(111) surface. (a) Typical STM image (a-i, 10 pA, 42 × 42 nm) and its zoom-in images for different phases (a-ii, phase B, 10 pA, 7 × 7 nm; a-iii, phase A, 100 pA, 6 × 6 nm) of the NDCAs on Cu(111) surface. (b) An overview STM image (b-i, 10 pA, 42 × 42 nm), as well its zoom-in images (b-ii and iii, 100 pA, 10 × 10 nm), of the NDCAs on Cu(111) surface after annealing to 120 °C. (c) Overview STM image (c-i, 10 pA, 170 × 170 nm), as well its zoom-in image (c-ii, 10 pA, 42 × 42 nm) and FFT pattern (c-iii, ±, 1.34, 1/nm), of the metallic polymerization products of NDCAs after further annealing to 160 °C. (d) High-resolution STM image (d,i, 10 pA, 12.5 × 12.5 nm) and its zoom-in images (d,ii, 100 pA, 4.24 × 4.24 nm; d,iii, 10 pA, 5 × 5 nm) of the C−Cu−C conjugations. (d,iv) Isomerized chemical structures of C−Cu−C conjugations were suggested. All the STM images were acquired at −2 V.

dx.doi.org/10.1021/ja5033875 | J. Am. Chem. Soc. 2014, 136, 9658−9663

parameters: a, 0.83 nm; b, 0.73 nm; angle 96.8° where the NDCA center-to-center distance was measured to be 1.16 ± 0.01 nm (see SI-Figure 4). R- and L-chiral NDCAs were separated in the ordered phase B (Figure 3a-ii). On the other hand, in the disordered phase A, NDCAs have a higher contrast, and the center-to-center distance was measured as 1.07 ± 0.01 nm, which matches three times that of the Cu(111) lattice. We believe that the carboxyl group as compared to the situation on Ag(111) and Au(111) surfaces is bending more downward to the Cu(111) surface.

Interestingly, after thermal annealing at 120 °C for 30 min we observed an intermediate state of NDCAs at Cu(111) without any covalent coupling between NDCAs (Figure 3b-i): unreacted NDCAs formed an ordered self-assembly phase (Figure 3b-ii), which looks similar to the ordered phase obtained on Ag(111) (see above). Isolated NDCAs and also NDCA-clusters were identified (Figure 3b-iii). Here, the isolated molecules were regarded as NDCAs chemical adsorbed at Cu surface via the dehydrogenation process (see structure in Scheme 1 after step 1, Cu atoms were not pulled out of the surface during metalation, which is different than for the reactions at Fe/Cu where Fe/Cu-carboxylic complexes were identified at the surface),[32] because unreacted NDCA monomers should either join the molecular self-assembly structure or desorb. Further annealing to 160 °C led to the formation of large poly-organometallic chains generated via the decarboxylative process (Figure 3c-i). The zoom-in image and the FFT pattern both demonstrate that the orientations of such metallic polymers were only along cooper ⟨110⟩, ⟨101⟩, and ⟨011⟩ directions (Figure 3c-ii and iii). This finding is an indication for the C−Cu−C linkage between naphthalenes, because of the interaction between Cu atoms of the poly-organometallic species with the Cu surface. As for the organo-silver intermediate discussed above, the C−Cu−C linkage appears with higher contrast in the image. Interestingly, successful STM manipulations of the oligo-bisnaphthyl-Cu species revealed the Cu−C bonds to have remarkable stability (SI-Figure 5).

Figure 3d,i depicts a representative high-resolution STM image of the C−Cu−C covalent bonding of NDCAs, in which few intermediate dehydrogenated surface bound NDCA monomers still exist. The NDCA center-to-center distance of the C−Cu−C type covalent coupling was measured as 0.89 ± 0.01 nm for both for R-to-R (L-to-L) and R-to-L conjugations. This indicates that the C−Metal−C functionality has a stronger interaction with the Cu(111) surface than with the Ag(111) surface. Theoretical calculations of the R-to-R (L-to-L) and R-to-L conjugations (NaphthylCu(I)Naphthyl) provided distances of 0.902 and 0.895 nm, respectively. This is in very good agreement with the experimentally determined values. Furthermore, bridges between NDCAs without direct covalent coupling were also identified as marked by a red cycle in Figure 3d,ii. The center-to-center distance for such a bridged structure was measured as 1.11 ± 0.04 nm, which suggests that the two NDCA molecules either interact via hydrogen bonding or are bridged via C−Cu−Cu−C type linkage. Based on the STM images, we currently believe that bridging via C−Cu−Cu−C is more likely (otherwise, the distance of such bridges varies much.).

Further annealing of the poly-organometallic naphthylenes on Cu(111) to 190.8 °C eventually provided poly-2,6-naphthalene. Figure 4a-i, shows a representative STM image (for large scale STM image, see SI-Figure 6). Along with the

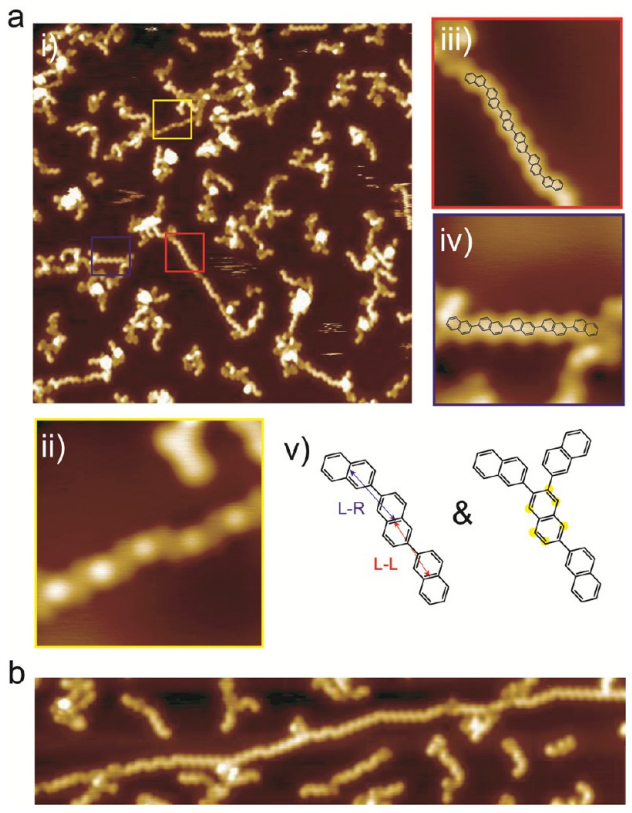

Figure 4. Final polymerization of NDCAs at Cu(111) surface. (a) An overview STM image (a-i, 10 pA, 42 × 42 nm) and its zoom-in images (a-ii and a-iii, 10 pA, 4.2 × 4.2 nm; a-iv, 10 pA, 5 × 5 nm) of the reaction products of NDCAs after annealing to 190.8 °C as well as the suggested chemical structures formed after covalent coupling a-v). (b) A typical STM image (100 pA, 50 × 9 nm) of a long poly-2,6-naphthalene. All STM images were acquired at −2 V.

poly-naphthalenes, some organometallic-polymers still remained (Figure 4a-ii). The ultrahigh-resolution STM image (Figure 4a-iii) reveals that the poly-naphthalene consists of both L-chiral and R-chiral moieties as drawn in the corresponding chemical structures in Figure 4a-v. The success of direct C−C covalent coupling was also proved by STM manipulations (SI-Figure 7). Moreover, the molecule center-to-center distance for the C−C covalent coupling was measured as 0.67 ± 0.02 nm for both R-to-R (L-to-L) and R-to-L couplings. In some cases, branching conjugations were also identified, as previously observed on Ag(111). It is important to point out that poly-2,6-naphthalene with a chain length of up to 50 nm was formed documenting the efficiency of the decarboxylative coupling under these conditions (Figure 4.b).

Cu(100) Surface Guided Polymerization of NDCAs. Encouraged by the results obtained on Cu(111) we finally investigated the on-surface polymerization of NDCAs on Cu(100) and Cu(110) surfaces. A different confinement toward the intermediate metallic polymers was expected such as illustrated in Figure 5a. The metal atoms that are part of the organometallic polymers should have a specific interaction with the metal surfaces.

For the Cu(100) case, we observed dehydrogenation of NDCAs after annealing up to 127 °C forming a NDCA-Cu-carboxylate coordination network (see SI-Figure 8).[32] Further annealing up to 160 °C led to the formation of organometallic polymers by formal decarboxylation. However, dehydrogenated

dx.doi.org/10.1021/ja5033875 | J. Am. Chem. Soc. 2014, 136, 9658−9663

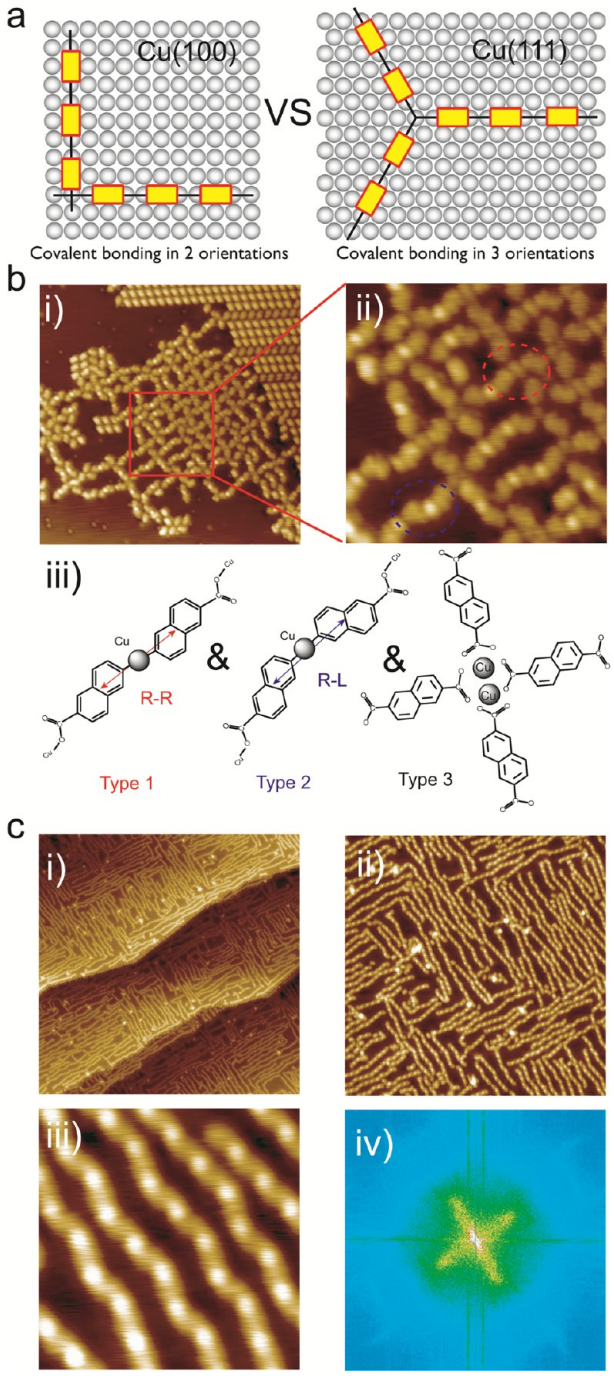

Figure 5. Substrates guided covalent couplings: Cu(100) vs Cu(111). (a) An illustration of the substrates guided covalent coupling in space. (b) Typical STM image (b-i, 200 pA, 25 × 25 nm) and zoom-in image (b-ii, 200 pA, 8 × 8 nm) of NDCAs at Cu(100) surface after annealing 160 °C. (b-iii) Suggested chemical structures for different conjugations among NDCAs at Cu(100) surface. (c) An overview STM image (c-i, 100 pA, 82 × 82 nm), a zoom-in image (c-ii, 100 pA, 42 × 42 nm) and a high-resolution STM image (c-iii, 100 pA, 6 × 6 nm) of the NDCA-metallic polymers on Cu(100) after annealing at 185.3 °C. (c-iv) The FFT pattern of (c-i) polymers (±, 2.68, 1/nm) was obtained. All the STM images were acquired at −0.5 V.

bisnaphthyl carboxylate species interacting with the substrate coexist as shown in Figure 5b-i. STM high-resolution image Figure 5.b-ii shows that the C−Cu−C bonding has a higher contrast than the coordination bonding in the metalated carboxylates, as well a shorter distance (center-to-center distance: C−Cu−C, 0.93 ± 0.03 nm; C(O)O−substrate−OCH(O), 1.25 ± 0.03 nm, for all R-to-R, L-to-L, R-to-L cases). The chemical structures of the different conjugations are suggested in Figure 5b-iii.

As expected, we found that the organometallic polymers were grown only in ⟨010⟩ and ⟨001⟩ directions of the Cu(100) surface (Figure 5c-i), after thermal treatment up to 185.3 °C. In the zoom-in image Figure 5c-ii, it is very interesting to observe that one long polymer can be bent by 90° along both ⟨010⟩ and ⟨001⟩ directions, which indicates the strong interaction between the metals of the C−Cu−C polymers and copper surfaces. Moreover, the C−Cu−C conjugations have a higher contrast than the naphthalene moieties, as also observed on Ag(111) and Cu(111) surfaces (Figure 5c-iii). The FFT pattern of polymers in Figure 5c-i, clearly shows the two-orientation symmetric in space distribution again (Figure 5c-iv). Poly-naphthalene via removing of Cu atoms was obtained at the Cu(100) surface after annealing up to 236 °C (see SI-Figure 9).

Finally, the Cu(110) surface was tested. We found that the covalent coupling of NDCAs starts to occur after annealing up to 206 °C, and short oligomers are formed after annealing up to 226 °C (see SI-Figure 10). However, all the chemical processes are occurring very fast at such higher temperatures, and polymeric organometallic intermediates were not observed. Based on previous reports on similar systems which did not reveal any decarboxylative C−C-coupling,[32] and our herein disclosed efficient couplings, we assume that reactions of COOH groups and organometallic intermediates derived therefrom, strongly depend on the molecular structure of the carboxylic acid and also on the substrate, especially when metal atoms of the substrate are actively involved in the individual steps of the coupling reactions.

3. CONCLUSIONS

In summary, we showed successful on-surface covalent coupling by using aromatic −COOH substituents as reactive moieties. If the arene is charged with two reactive hydroxycarbonylsubstituents, such as in NDCA, the on-surface reaction leads to the formation of polymeric structures. Based on STM characterized reaction intermediates, a possible mechanism for the polymerization was suggested. Reactions occur via initial H-bonding self-assembly of NDCA with subsequent formation of metal carboxylates upon annealing. Further increase of the reaction temperature leads via decarboxylation to the formation of polymeric bisnaphthyl-metal intermediates which upon further annealing undergo reductive elimination to eventually provide poly-naphthalenes. The efficiency of the decarboxylative coupling of NDCA to give poly-naphthalene strongly depends on the substrate. The following reactivity order was observed: Cu(111) > Cu(100) > Ag(111) > Cu(110) > Au(111), which relates to the reduction−oxidation ability of the metal and likely the ability of metal atoms being pulling out of the surface.

■ ASSOCIATED CONTENT

Ⓢ Supporting Information

More detailed descriptions of the STM experiments and analysis. This material is available free of charge via the Internet at http://pubs.acs.org.

■ AUTHOR INFORMATION

Corresponding Authors

gaoh@uni-muenster.de

dx.doi.org/10.1021/ja5033875 | J. Am. Chem. Soc. 2014, 136, 9658−9663

studer@uni-muenster.de
fuchsh@uni-muenster.de

Notes

The authors declare no competing financial interest.

■ ACKNOWLEDGMENTS

We thank the Deutsche Forschungsgemeinschaft (SFB 858 and TRR 61) for financial support. H.-Y.G. was supported by the Alexander von Humboldt Foundation.

■ REFERENCES

(1) Gourdon, A. *Angew. Chem., Int. Ed.* **2008**, *47*, 6950−6953.
(2) Perepichka, D. F.; Rosei, F. *Science* **2009**, *323*, 216−217.
(3) Elemans, J. A. A. W.; Lei, S.; De Feyter, S. *Angew. Chem., Int. Ed.* **2009**, *48*, 7298−7333.
(4) Palma, C.-A.; Samori, P. *Nat. Chem.* **2011**, *3*, 431−436.
(5) Sakamoto, J.; von Heijst, J.; Lukin, O.; Schlüter, A. D. *Angew. Chem., Int. Ed.* **2009**, *48*, 1030−1069.
(6) Colson, J. W.; Dichtel, W. R. *Nat. Chem.* **2013**, *5*, 453−465.
(7) Björk, J.; Hanke, F. *Chem.—Eur. J.* **2014**, *20*, 928−934.
(8) Lafferentz, L.; Ample, F.; Yu, H.; Hecht, S.; Joachim, C.; Grill, L. *Science* **2009**, *323*, 1193−1197.
(9) Wang, W.; Shi, X.; Wang, S.; Van Hove, M. A.; Lin, N. *J. Am. Chem. Soc.* **2011**, *133*, 13264−13267.
(10) Cai, J.; Puffieux, P.; Jaafar, R.; Bieri, M.; Braun, T.; Blankenburg, S.; Muoth, M.; Seitsonen, A. P.; Saleh, M.; Feng, X.; Müllen, K.; Fasel, R. *Nature* **2010**, *466*, 470−473.
(11) Linden, S.; Zhong, D.; Timmer, A.; Aghdassi, N.; Franke, J.-H.; Zhang, H.; Feng, X.; Müllen, K.; Fuchs, H.; Chi, L.; Zacharias, H. *Phys. Rev. Lett.* **2012**, *108*, 216801−216806.
(12) Grill, L.; Dyer, M.; Lafferentz, L.; Persson, M.; Peters, M. V.; Hecht, S. *Nat. Nanotechnol.* **2007**, *2*, 687−691.
(13) Bieri, M.; Nguyen, M.-T.; Gröning, O.; Cai, J.; Treier, M.; Aït-Mansour, K.; Ruffieux, P.; Pignedoli, C. A.; Passerone, D.; Kastler, M.; Müllen, K.; Fasel, R. *J. Am. Chem. Soc.* **2010**, *132*, 16669−16676.
(14) Gutzler, R.; Walch, H.; Eder, G.; Kloft, S.; Heckl, W. M.; Lackinger, M. *Chem. Commun.* **2009**, 4456−4458.
(15) Weigelt, S.; Busse, C.; Bombis, C.; Knudsen, M. M.; Gothelf, K. V.; Strunskus, T.; Wöll, C.; Dahlbom, M.; Hammer, B.; Lægsgaard, E.; Besenbacher, F.; Linderoth, T. R. *Angew. Chem., Int. Ed.* **2007**, *46*, 9227−9230.
(16) Weigelt, S.; Busse, C.; Bombis, C.; Knudsen, M. M.; Gothelf, K. V.; Lægsgaard, E.; Besenbacher, F.; Linderoth, T. R. *Angew. Chem., Int. Ed.* **2008**, *47*, 4406−4410.
(17) Liu, X.-H.; Guan, C.-Z.; Ding, S.-Y.; Wang, W.; Yan, H.-J.; Wang, D.; Wan, L.-J. *J. Am. Chem. Soc.* **2013**, *135*, 10470−10474.
(18) Zwaneveld, N. A. A.; Pawlak, R.; Abel, M.; Catalin, D.; Gigmes, D.; Bertin, D.; Porte, L. *J. Am. Chem. Soc.* **2008**, *130*, 6678−6679.
(19) Matena, M.; Riehm, T.; Stähr, M.; Jung, T. A.; Gade, L. H. *Angew. Chem., Int. Ed.* **2008**, *47*, 2414−2417.
(20) Treier, M.; Richardson, N. V.; Fasel, R. *J. Am. Chem. Soc.* **2008**, *130*, 14054−14055.
(21) Marele, A. C.; Mas-Ballesté, R.; Terracciano, L.; Rodríguez-Fernández, J.; Berlanga, I.; Alexandre, S. S.; Otero, R.; Gallego, J. M.; Zamora, F.; Gómez-Rodríguez, J. M. *Chem. Commun.* **2012**, *48*, 6779−6781.
(22) Bebensee, F.; Bombis, C.; Vadapoo, S.-R.; Cramer, J. R.; Besenbacher, F.; Gothelf, K. V.; Linderoth, T. R. *J. Am. Chem. Soc.* **2013**, *135*, 2136−2139.
(23) Díaz Arado, O.; Mönig, H.; Wagner, H.; Franke, J.-H.; Langewisch, G.; Held, P. A.; Studer, A.; Fuchs, H. *ACS Nano* **2013**, *7*, 8509−8515.
(24) Sun, Q.; Zhang, C.; Li, Z.; Kong, H.; Tan, Q.; Hu, A.; Xu, W. *J. Am. Chem. Soc.* **2013**, *135*, 8448−8451.
(25) Zhong, D.; Franke, J.-H.; Podiyanachari, S. K.; Blömker, T.; Zhang, H.; Kehr, G.; Erker, G.; Fuchs, H.; Chi, L. *Science* **2011**, *334*, 213−216.
(26) Zhang, Y.-Q.; Kepčija, N.; Kleinschrodt, M.; Diller, K.; Fischer, S.; Papageorgiou, A. C.; Allegretti, F.; Björk, J.; Klyatskaya, S.; Klappenberger, F.; Ruben, M.; Barth, J. V. *Nat. Commun.* **2012**, *3*, 1286−1293.
(27) Gao, H. Y.; Wagner, H.; Zhong, D.; Franke, J.-H.; Studer, A.; Fuchs, H. *Angew. Chem., Int. Ed.* **2013**, *52*, 4024−4028.
(28) Gao, H. Y.; Franke, J.-H.; Wagner, H.; Zhong, D.; Held, P. A.; Studer, A.; Fuchs, H. *J. Phys. Chem. C* **2013**, *117*, 18595−18602.
(29) Cirera, B.; Zhang, Y.-Q.; Klyatskaya, S.; Ruben, M.; Klappenberger, F.; Barth, J. V. *Chem. Catal. Chem.* **2013**, *5*, 3281−3288.
(30) Saywell, A.; Schwarz, J.; Hecht, S.; Grill, L. *Angew. Chem., Int. Ed.* **2012**, *51*, 5096−5100.
(31) Björk, J.; Hanke, F.; Stafström, S. *J. Am. Chem. Soc.* **2013**, *135*, 5768−5775.
(32) (a) Kley, C. S.; Čechal, J.; Kumagai, T.; Schramm, F.; Ruben, M.; Stepanow, S.; Kern, K. *J. Am. Chem. Soc.* **2012**, *134*, 6072−6075. (b) Langner, A.; Tait, S. L.; Lin, N.; Rajadurai, C.; Ruben, M.; Kern, K. *Proc. Natl. Acad. Sci. U. S. A.* **2007**, *104*, 17927−17930. (c) Spillmann, H.; Dmitriev, A.; Lin, N.; Messina, P.; Barth, J. V.; Kern, K. *J. Am. Chem. Soc.* **2003**, *125*, 10725−10728. (d) Lin, N.; Payer, D.; Dmitriev, A.; Strunskus, T.; Wöll, C.; Barth, J. V.; Kern, K. *Angew. Chem., Int. Ed.* **2005**, *44*, 1488−1491. (e) Seitsonen, A. P.; Lingenfelder, M.; Spillmann, H.; Dmitriev, A.; Stepanow, S.; Lin, N.; Kern, K.; Barth, J. V. *J. Am. Chem. Soc.* **2006**, *128*, 5634−5635. (f) Barth, J. V. *Annu. Rev. Phys. Chem.* **2007**, *58*, 375−407.
(33) Lafferentz, L.; Eberhardt, V.; Dri, C.; Africh, C.; Comelli, G.; Esch, F.; Hecht, S.; Grill, L. *Nat. Chem.* **2012**, *4*, 215−220.
(34) (a) Myers, A. G.; Tanaka, D.; Mannion, M. R. *J. Am. Chem. Soc.* **2002**, *124*, 11250−11251. (b) Tanaka, D.; Romeril, S. P.; Myers, A. G. *J. Am. Chem. Soc.* **2005**, *127*, 10323−10333. (c) Forgione, P.; Brochu, M.-C.; St-Onge, M.; Thesen, K. H.; Bailey, M. D.; Bilodeau, F. *J. Am. Chem. Soc.* **2006**, *128*, 11350−11351. (d) Gooßen, L. J.; Deng, G. J.; Levy, L. M. *Science* **2006**, *313*, 662−664. (e) Gooßen, L. J.; Rodríguez, N.; Gooßen, K. *Angew. Chem., Int. Ed.* **2008**, *47*, 3100−3120. (f) Rodríguez, N.; Gooßen, L. J. *Chem. Soc. Rev.* **2011**, *40*, 5030−5048. (g) Weaver, J. D.; Recio, A., III; Grenning, A. J.; Tunge, J. A. *Chem. Rev.* **2011**, *111*, 1846−1913. (h) Cornella, J.; Larrosa, I. *Synthesis* **2012**, *44*, 653−676. (i) Dzik, W. I.; Lange, P. P.; Gooßen, L. J. *Chem. Sci.* **2012**, *3*, 2671−2678. (j) Ruhland, K. *Eur. J. Org. Chem.* **2012**, 2683−2706.
(35) Clair, S.; Pons, S.; Seitsonen, A. P.; Brune, H.; Kern, K.; Barth, J. V. *J. Phys. Chem. B* **2004**, *108*, 14585−14590.